Lawrence Berkeley National Laboratory
LBL Publications

Title
STM STUDY OF THE STRUCTURE OF THE SULFUR (1X2) OVERLAYER ON MOLYBDENUM (001) IN AIR: ORDERED DOMAINS, PHASE BOUNDARIES AND DEFECTS

Permalink
https://escholarship.org/uc/item/0rw495sh

Authors
Marchon, B.
Ogletree, D.F.
Bussell, M.E.

Publication Date
1988-07-01

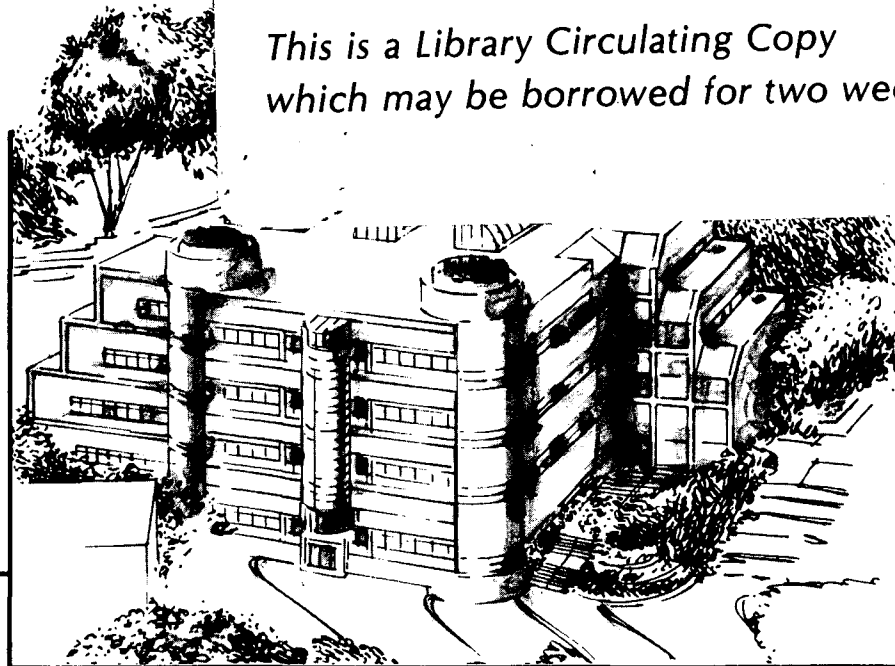**Center for Advanced Materials**

CAM

STM Study of the Structure of the Sulfur (1×2) Overlayer on Molybdenum (001) in Air: Ordered Domains, Phase Boundaries and Defects

B. Marchon, D.F. Ogletree, M.E. Bussell, G.A. Somorjai,
M. Salmeron, and W. Siekhaus

July 1988

Materials and Chemical Sciences Division

Lawrence Berkeley Laboratory • University of California

ONE CYCLOTRON ROAD, BERKELEY, CA 94720 • (415) 486-4755

DISCLAIMER

STM STUDY OF THE STRUCTURE OF THE SULFUR (1×2) OVERLAYER ON MOLYBDENUM (001) IN AIR: ORDERED DOMAINS, PHASE BOUNDARIES AND DEFECTS

B. Marchon[†], D.F. Ogletree, M.E. Bussell , G.A. Somorjai, M. Salmeron[*]
and W. Siekhaus[1].
Center for Advanced Materials
Lawrence Berkeley Laboratory, Berkeley, CA 94720
and
[1] Lawrence Livermore National Laboratories, Livermore, CA 94550.

† Permanent address: Laboratoire de Spectrochimie Infrarouge et Raman, CNRS, 94320 Thiais, France.
* To whom correspondence should be addressed.

ABSTRACT

A (001) surface of molybdenum, covered by one monolayer of sulfur was prepared in UHV and characterized by LEED, Auger and XPS. This surface was found to be stable in air for periods of several days. STM images of the surface, obtained in air in the topographic and local barrier height modes, revealed the atomic arrangement of sulfur atoms in domains with 1×2 and 2×1 periodicities. Boundaries between domains, adsorbate and substrate defect structures and crystallites formed during the initial oxidation of the Mo substrate were observed.

1 Introduction

The surfaces of molybdenum with adsorbed layers of sulfur has been used to model the catalysts that remove sulfur from hydrocarbon molecules, Gellman et al. (1984). LEED studies show that sulfur forms several ordered structures on the (001) face of Mo as a function of coverage, Clarke, (1981), Salmeron et al. (1983). Like all diffraction techniques, LEED is best suited to study those structures that form long range ordered domains. Defect structures, anti-phase domain boundaries and disordered regions escape detection in most cases, while they might dominate the surface reactivity. The scanning tunneling microscope (STM) is ideally suited to study the local structure of the surface, including the non-periodic structures mentioned above. In addition the STM can be operated in atmospheric pressure environments, a condition that can be of crucial importance for catalytic studies of surfaces.

In this paper we will show the structures formed in ultra-high vacuum (UHV) by a saturation monolayer of sulfur on Mo(001) and observed by STM at atmospheric pressure. The ordered parts of this layer form domains with 1×2 and 2×1 periodicities in accordance with the LEED observations. This result was the object of a recent letter, Marchon et al.

3

(1988a), in which a model for the sulfur structure was proposed consistent of equivalent sites half way between the bridge and four-fold positions. We present now a more extensive account of our studies that include, in addition to these ordered structures, others that are non-periodic like domain and grain boundaries.

2 Experimental

The Mo(001) surface was prepared by standard metallographic techniques and oriented by Laue X-ray diffraction. The crystal was cleaned in UHV by sputtering and oxygen treatments followed by high temperature annealing. A saturation coverage of sulfur was subsequently deposited by either a molecular beam of S_2 from the electrochemical decomposition of Ag_2S, Salmeron et al. (1983), or by exposure to H_2S. The saturation coverage corresponds to one monolayer (one sulfur atom per top-layer molybdenum atom), according to previous LEED and Auger studies, Gellman et al. (1984), Clarke (1981). The LEED pattern at this stage showed extra spots characteristic of 1×2 and 2×1 periodicities. Small amounts of Carbon impurities were also present.

The crystal was then removed from the UHV chamber and installed in an STM that operates in air. This microscope consists of a tripod arrange-

ment of piezoelectric elements that support the tunneling tip. The tips used in this study were prepared by mechanically cutting a 1 mm diameter Pt-Rh (60 : 40%) alloy wire without any further treatment. The sample was mechanically positioned within the range of the Z-piezo feedback by two micrometers that bend an asymmetric bar supporting the sample.

The imaging conditions were as follows. A bias voltage between +50 and -50 mV was applied to the sample at a gap resistance between 2 and 20 megohms, with typical tunnel currents of 2 to 15 nA. Images composed of 128 lines of 256 data points each were recorded with a tip velocity of 650 Å per second giving an image acquisition time between 30 and 100 seconds. Images obtained at different bias voltages (below 0.2 volts), polarities and gap resistance, were similar.

Two methods of imaging were employed. The first one is the topographic mode that is commonly used in STM. In this mode, the tunneling current is kept constant and the topography of the surface charge density contour is displayed. The second method is the local barrier height mode. In this mode, the tip to surface gap distance is modulated at a frequency above the feedback loop cut-off, so that the mean value of the tunneling current is maintained constant. The amplitude of the AC component of the instantaneous tunnel current, as measured by a lock-in amplifier, is related to the square root of the local barrier height. According to the simple model

currently utilized, the tunneling current I_t is related to the gap distance s and the barrier height ϕ through the simple expression:

(1)
$$I_t \propto e^{-\lambda\sqrt{\phi}s}$$

For $s = s_0 + \delta(s)cos(\omega t)$, the amplitude $\delta(I)$ of the first harmonic of I_t becomes:

$$\delta(I) = -\lambda I_t^0 \delta(s)\sqrt{\phi}$$

Measuring $\delta(I)$ at each point for a given $\delta(s)$ and I_t^0, produces the barrier height image. The modulation amplitude $\delta(s)$ used in our experiments was between 0.2 and 0.6 Å, and the modulation frequency was at or above 4 KHz.

It must be emphasized that the signal obtained in this way might contain some contribution of the local topography as Binnig et al. have pointed out, Binning et al. (1986). In our case, however, the maximum slope in the topographs around the sulfur atoms is less than 12 degrees, as shown in figure 4. Therefore, the topographic contribution to the barrier height images can be estimated to be 2%, i.e. negligible. In addition, this influence would appear at twice the frequency of the atomic corrugation, contrary to our observations.

The local barrier height imaging mode, which involves an AC synchronous detection, has the inherent advantage of providing a higher signal-

to-noise ratio than a DC measurement as performed in the topographic mode.

3   Stability of the S-covered Mo(001) surface

After the surface was dosed with sulfur to saturation, the Auger spectrum was obtained and is shown in the upper part of figure 1. The main peak corresponds to sulfur at 148 eV. Molybdenum produces peaks at 120, 186 and 220 eV. A small residual peak of Carbon at 272 eV is also present that corresponds to less than 0.3 monolayers, Salmeron et al. (1983). The LEED pattern corresponding to this layer is shown in the upper part of figure 2 and shows the two sets of extra spots characteristic of the 1×2 and 2×1 domains.

To investigate the stability of the surface to oxidation and contamination in air, we opened the vacuum chamber to the atmosphere for a period of 14 hours while the crystal remained on the manipulator. After this time the system was pumped down and without further treatment the surface was examined by LEED and Auger Spectroscopy. The results of this experiment are shown in the lower part of figures 1 and 2. The LEED pattern shows no discernible change while the Auger spectrum indicates an increase in the amount of Carbon to about 0.5 monolayers. Oxygen is

also present in amounts below 0.25 monolayers, Salmeron et al. (1983), as judged from the small peak at around 510 eV. No change in the relative amounts of sulfur and molybdenum were observed.

In spite of the C and O contaminants, this experiment shows very clearly the remarkable protection that one monolayer of sulfur imparts to the very reactive molybdenum surface. As we shall see, our STM results further confirm this observation. For longer exposures to the atmosphere, the degree of contamination by C and O increases. Clearly the oxide is more stable thermodynamically, and only the kinetics of the oxidation have been slowed down by the sulfur monolayer. X-Ray Photoelectron Spectroscopy (XPS) examination showed that some samples had more oxygen than sulfur on the surface after several days exposure to air. Mo(001) surfaces with lower sulfur coverages oxidize rapidly, even the ordered c(2×4) structure with a sulfur coverage of 0.75 monolayers that completely blocks chemisorption in UHV, Salmeron et al. (1983). We propose that the oxide nucleates and grows from the defects in the sulfur monolayer that expose the molybdenum substrate atoms. The STM studies in air were performed in surfaces passivated by a full monolayer of sulfur.

4 The ordered 1×2 domains

In figure 3 we show a barrier height image of a 40×25 Å region. The pseudo hexagonal arrangement of bright spots has the 1×2 symmetry of the sulfur overlayer which was observed by LEED in vacuum. The shortest atom-atom distance in this image is 3.4 Å, which, within the precision of the piezo calibration, corresponds to the molybdenum-molybdenum lattice distance of 3.14 Å along the [100] direction. In other regions of the crystal the pattern was rotated by 90 degrees, corresponding to 2×1 domains. Single scan profiles along the rows of sulfur atoms in the [100] and [120] directions are reproduced in figures 4a and 4b. The width of the corrugation peaks is approximately equal to 1.4 Å, which is indicative of the lateral resolution achieved in this experiment. The images taken in the topographic mode had a lower signal to noise ratio than those taken in the barrier height mode. An example is shown in figure 5. Topographic line profiles through the rows of sulfur atoms along the [010] and the [120] directions are shown in figures 4c and 4d. The width of the corrugation peaks in this case is also close to 1.5 Å. The vertical corrugation in both directions is approximately 0.4 Å.

Clarke proposed a structural model in which sulfur atoms occupy two- and four-fold sites, as shown in model I in the lower part of figure 4. However, as this author pointed out, a displacement by a quarter of a unit cell along the [100] axis produces a structure where all sulfur atoms

9

occupy equivalent sites (model II). This structure would give rise to the same LEED pattern. Such bonding sites can be viewed as three-fold sites, taking into account the second layer of molybdenum atoms. Our results seem to favor the latter model, in view of the uniform corrugation that is observed along the [120] direction, for either type of imaging. In model I, the [120] direction has sulfur atoms in alternating bridge and four-fold hollow sites. This would lead, in a hard-sphere model, to a variation close to 0.8 Å for the heights of two-fold and four-fold sulfur atoms. Our line profile measurements along the [120] direction, shown in figure 4d, show a height difference not greater than 0.1· Å for the two kind of sulfur atoms. This conclusion must however, be taken with some caution, as the line profiles show the corrugation of the local density of states at the Fermi level at some distance from the surface. As discussed in our previous account of this work, Marchon et al. (1988a), the bright, high barrier height spots in the images, are attributed to the top of the sulfur atoms.

5 Imperfections in the surface layer

Not all of the crystal surface showed a uniform and perfect 1×2 periodicity. Many areas of the crystal surface produced noisy and disordered images, particularly after long air exposures. We attribute this to contam-

ination and oxidation.

In addition to this, we observed a variety of "imperfections" including domain boundaries between 1×2 and 2×1 regions, antiphase boundaries between two 1×2 (or 2×1) domains, and localized regions showing 1×1 arrangements. Striking intensity modulations in the images were also observed that produced a structure of parallel stripes, one unit cell wide. Finally, we show an image of a region with a small angle grain boundary.

5.1 Domain boundaries

Coexisting 1×2 and 2×1 domains are often observed in the same STM image. 2×1 domains are seen in the upper part of Figure 6, with the short side of the unit cell running approximately along a diagonal from the upper left to the lower right corner of the figure. In the lower part of figure 6, 1×2 domains can be seen. Now the short side of the unit cell is along the diagonal from the lower left to upper right.

Figure 7 shows a more detailed image of the boundary between a 2×1 and a 1×2 region. The registry of these two domains helps distinguish between the proposed models for the sulfur overlayer illustrated in figure 4.

In model I sulfur atoms occupy inequivalent bridge and 4-fold hollow sites. At a domain boundary the long side of the 2×1 and the short side

11

of the 1×2 should be colinear, and there should be a registry shift of half a lattice spacing.

In model II, sulfur atoms are adsorbed in equivalent quasi-3-fold sites in contact with two top-layer atoms and one second-layer molybdenum atom. These sites are displaced horizontally by one quarter of a lattice spacing from the bridge site axis. At a domain boundary the long side of the 2×1 and the short side of the 1×2 unit cells should be displaced by one half of a lattice spacing, and there should be a registry shift of one quarter of a lattice spacing.

In figure 7 the distance between the closest visible unit cell edges in these two domains is 3.30 ± 0.05 lattice constants. In addition there is a parallel shift along the domain boundary of between 0.5 and 0.25 lattice constants. These observations support model II of figure 4, in accordance with our previous conclusions based on the corrugation profile (see figure 4).

Another possibility is the presence of an atomic step separating the two domains. The observed decrease in local barrier height between the two domains could be consistent with such a possibility. Localized decreases of barrier height in the vicinity of step edges were clearly observed in our studies of sulfur on Re(0001), Marchon et al. (1988b). In this case the observed separation and shift along the boundary would be compatible with

either model. However, we believe that this interpretation is not correct since the dark area of low barrier height comes to an end near the top of the figure.

Some regions of the crystal surface showed modulations in intensity that formed patterns of parallel stripes, typically one 2×1 unit cell wide and separated by 1, 2 or 3 lattice constants. The direction of the stripes is always parallel to the ×1 direction of the 1×2 periodicity. Examples of this are shown in figures 8 and 9. This pattern is observed in both topographic and barrier height images, and the stripe corrugation observed in the topographic scans is 1 Å or less. The modulation in intensity that gives rise to the striped pattern is not understood at present.

Figure 8 shows antiphase boundaries separating a 2×1 domain from a narrow stripe of 1×1 unit cells. The model drawn in the lower part of the figure is compatible with the observed separation of 1.25 lattice spacings across the boundary, and with the shift in the vertical direction. Antiphase boundaries with 1×1 sulfur structure are also observed in other images.

5.2 Low Angle Grain Boundaries

The region of the crystal shown in figure 9 is covered with sulfur in a 2×1 orientation. Two domains are clearly visible that fill the upper half

13

and the lower half of the image. Both domains show the striped discussed in the last section. The boundaries of the stripes are marked by the lines running more or less vertically. The horizontal lines mark some unit cells and also indicate the angle of mismatch between the two domains. This angle is equal to 7°.

We can explain this observation by assuming that the sulfur is following the substrate structure and that the molybdenum substrate is composed of grains with low angle boundaries. This type of structure can appear in a single crystal as a result of mechanical strain during preparation. To our knowledge, this is the first real space observation of this type of defect on the surface of a crystal. Other authors, Welkie et al. (1980), have observed substrate defects with LEED that were attributed to such mosaic structures.

6   Formation of molybdenum oxide

Even sulfur passivated molybdenum crystals eventually oxidize when kept in air for extended periods. Once oxidation begins, three-dimensional molybdenum oxide crystallites are formed. After our STM observation were complete, we were able to detect molybdenum oxide with XPS.

Figure 10 shows surface features aligned along the [100] and [010]

directions that we attribute to the initial stages of molybdenum oxidation. Their size is typically 15 Å by 5 to 10 Å. The surface roughness is on the order of 10 to 20 Å.

7 Conclusions

Our work on the structure of sulfur covered Mo(001) surfaces can be summarized as follows:

1. The Mo(001) surface can be protected from contamination and oxidation in air, for periods ranging from hours to days, by one single atomic layer of sulfur.

2. Atomically resolved images of the 1×2 structure can be obtained in air by STM with excellent resolution. The observed corrugation due to the sulfur atoms is 0.4 Å, and the heights of neighboring atoms are within 0.1 Å of one another.

3. A variety of defects and non periodic structures have been observed in the overlayer, including domain boundaries and low angle grain boundaries, which must reflect underlying substrate defects.

4. The initial oxidation of molybdenum forms elongated crystallites of approximately 10 Å size oriented along the [100] direction.

ACKNOWLEDGEMENTS

16

REFERENCES

Binnig, G. & Rohrer, H. (1986)

Scanning Tunneling Microscopy. *IBM J. Res. and Dev.* 30, 355-369.

Clarke, L.J. (1981)

Structure of S Adsorbed on Mo(001) by LEED Analysis; Effects on CO Adsorption. *Surf. Sci.* 102, 331-347.

Gellman, A.J., Farias, M.H. & Somorjai, G.A. (1984)

The Catalytic Hydrodesulfurization of Thiophene on the Mo(100) crystal Surface. *J. of Catalysis* 88, 546-548.

Marchon, B., Bernhardt, P., Bussell, M.E., Somorjai, G.A., Salmeron, M. & Siekhaus, W. (1988a)

Atomic Arrangement of Sulfur Adatoms on Mo(001) at Atmospheric Pressure: A Scanning Tunneling Microscopy Study. *Phys. Rev. Letters*, 60, 1166-1169.

Marchon, B., Ogletree, D.F., Salmeron M. & Siekhaus, W. (1988b)

Scanning tunneling microscopy study of the Re(0001) surface passivated by one-half a monolayer of sulfur in an atmospheric environment. *J. Vac. Sci. & Technol.* A, 6, 531-533.

Salmeron, M., Somorjai, G.A. & Chianelli, R.R. (1983)

A LEED-AES Study of the Structure of Sulfur Monolayers on the Mo(100) Crystal Face. *Surf. Sci.* **127**, 526-540.

Welkie, D.G., Lagally, M.G. & Palmer, R.L. (1980)

Low-Energy electron diffraction study of the surface defect structure of Ag(111) epitaxially grown on mica. *J. Vac. Sci. & Technol.* **17**, 453-457.

FIGURE CAPTIONS

1. Auger electron spectra of the sulfur passivated Mo(001) surface before and after exposure to air. There are no significant changes in the Mo and S peaks after exposure, and only a small increase in the carbon peak at 272 eV.

2. Low energy electron diffraction patterns of the Mo(001)-(2×1)-S overlayer before and after exposure to air. Contributions from domains of (1×2) and (2×1) unit cells are superimposed in the observed LEED pattern.

3. An STM image, recorded in the local barrier height mode, of an ordered region of the Mo(001)-(1×2)-S overlayer. The long side of the (1×2) unit cell is vertical. The image size is 40×25Å.

4. The top half of the figure shows cross-sections through the sulfur atoms along the [100] and [120] directions in both local barrier height and topographic modes. In the lower half, two possible models for the Mo(001)-(2×1)S overlayer are shown: In model I one atom in each unit cell is located in a four-fold hollow site and the second is in a two-fold bridge site. In model II the two sulfur atoms are adsorbed in equivalent quasi-3-fold sites in contact with two top-layer atoms and one second-layer molybdenum atom.

5. An 80×80 Å topographic STM image of the Mo(001)-(1×2)-S over-layer. An ordered region can be seen in the lower right part of the figure.

6. An 80×80 Å local barrier height STM image of the Mo(001)-(2×1)-S overlayer. In the upper part the image (2×1) domains are seen, with the short side of the unit cell running along a diagonal from the upper left to the lower right corner of the figure. In the lower part of the figure (1×2) domains can be seen. Now the short side of the unit cell is along the diagonal from the lower left to upper right.

7. The upper half of the figure is an STM close-up of a domain boundary between (2×1) and (1×2) regions, taken in the local barrier height mode. The lower half of the figure is a schematic of the preferred geometry.

8. A domain boundary between a (2×1) region and a small area of (1×1) order is shown. Although not observed in LEED, small areas of (1×1) unit cells are frequently seen in the STM images. A schematic drawing of this regions is shown in the lower half of the figure.

9. An 50×50 Å local barrier height STM image of the Mo(001)-(2×1)-S overlayer. There is an angular mis-orientation between the upper and lower halves of the image due to a small-angle grain boundary

in the molybdenum substrate, as indicated by the solid lines. The vertical lines indicate the "striped" intensity modulation discussed in the text. This feature can also be seen in figures 7 and 8.

10. An 80×80 Å topographic STM image of an oxidized region of the molybdenum surface. The crystallites are oriented along the [100] and [010] directions. The corrugation is approximately 20 Å.
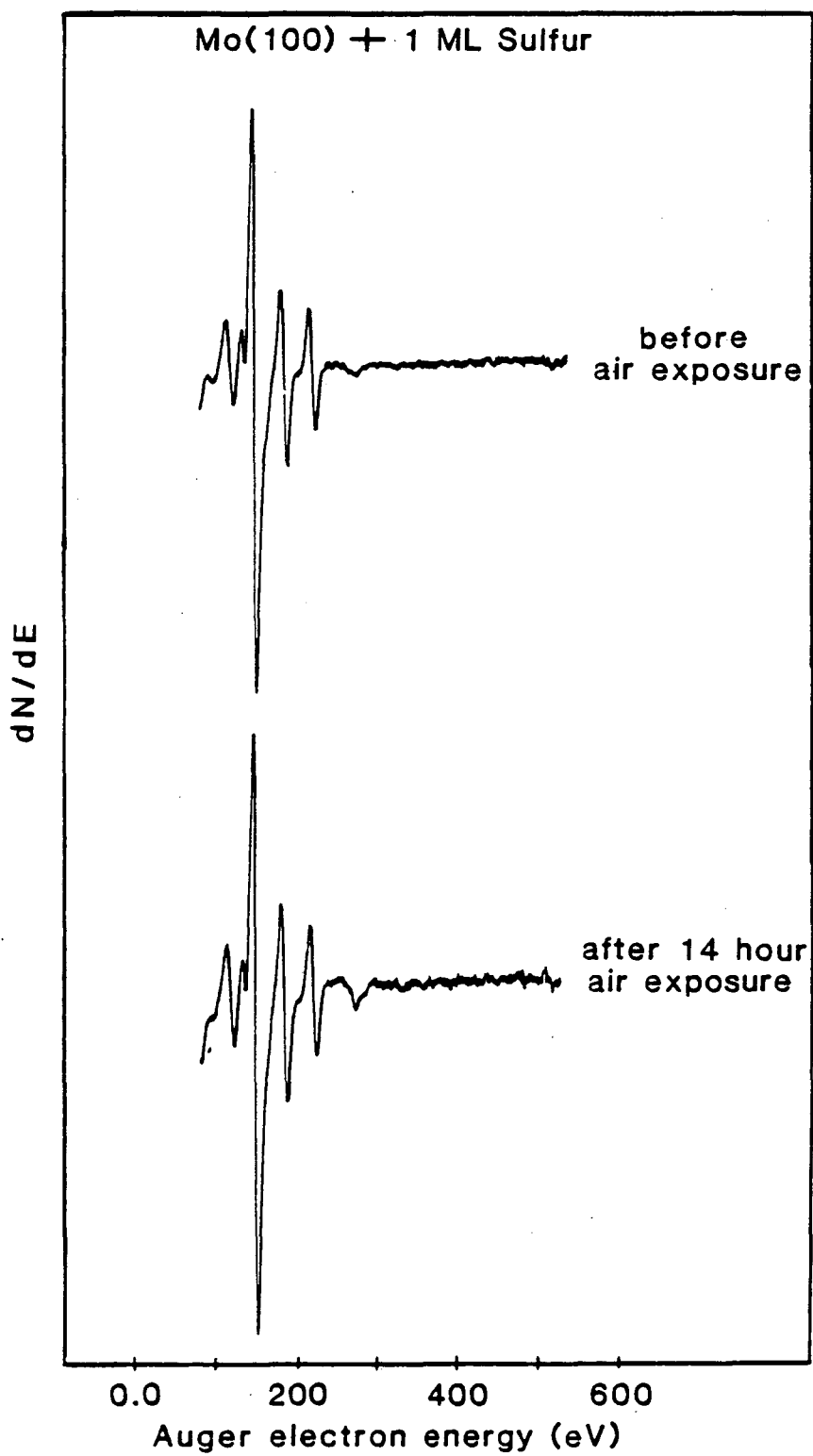
Fig. 1

XBL 886-2296

Mo(100) + 1 ML Sulfur
p(2 x 1) LEED Pattern

before
air exposure
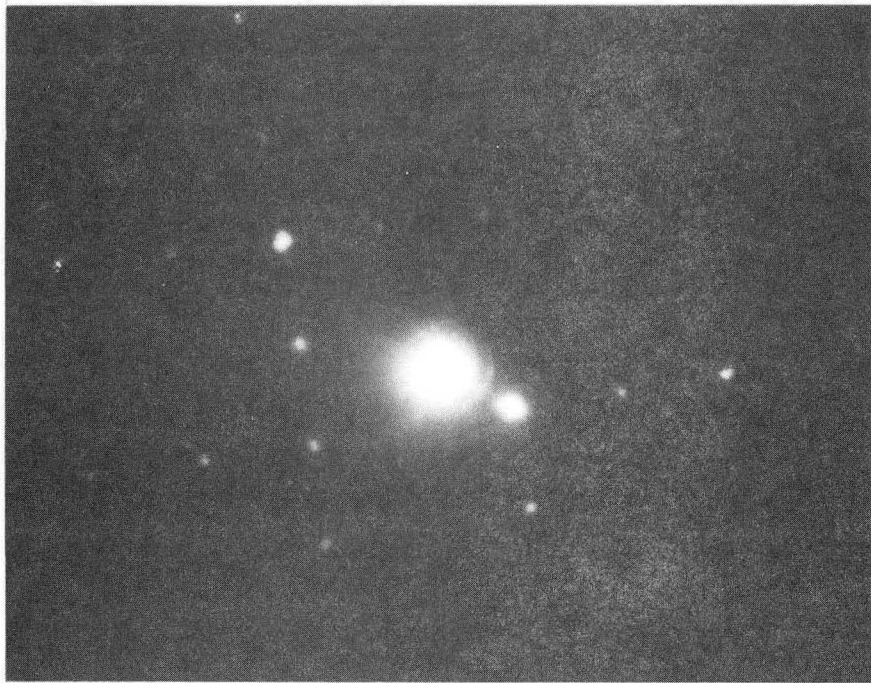
after 14 hour
air exposure

XBB 870-8292

beam energy = 125 eV

Fig. 2
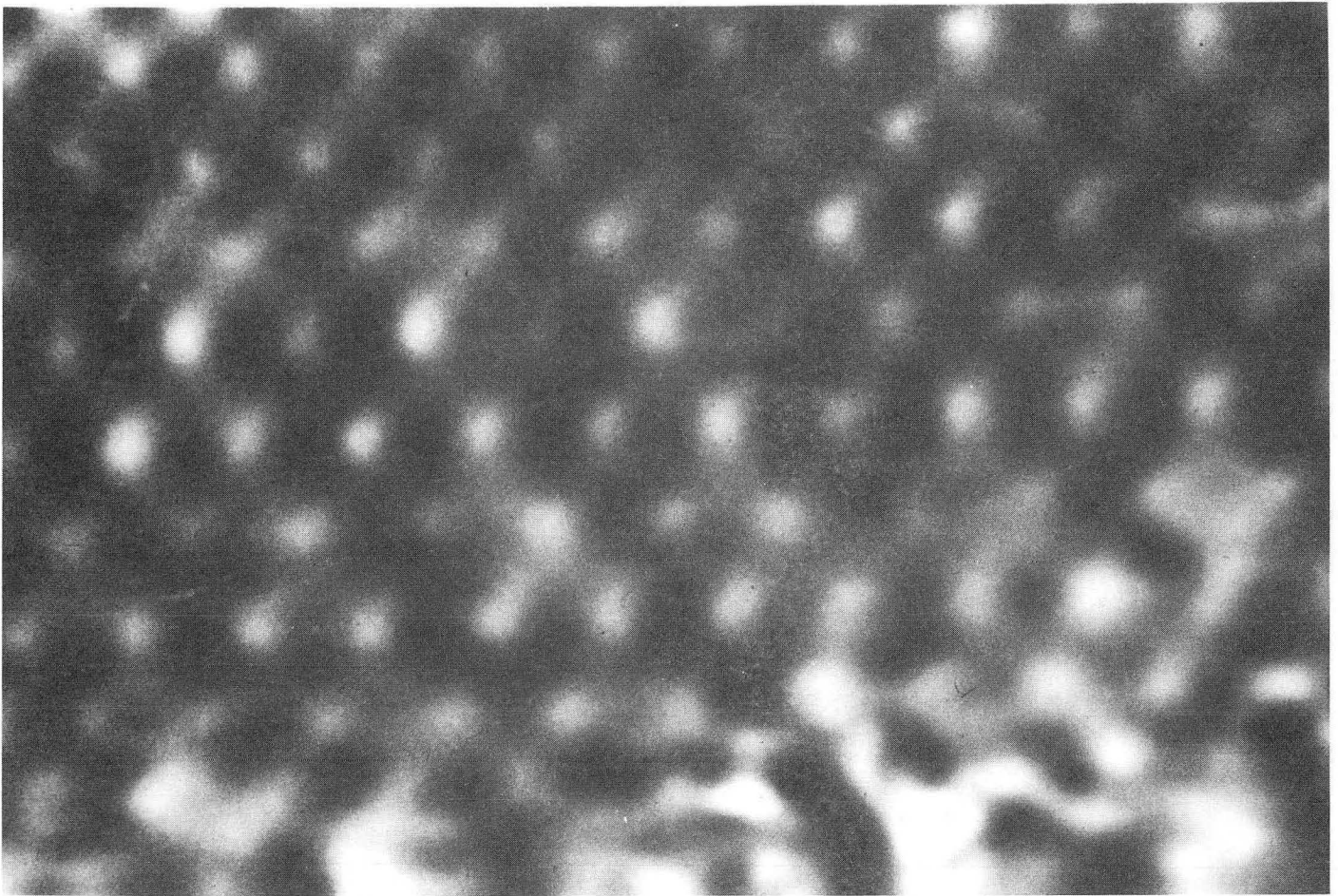
Fig. 3

Experimental line scan profiles
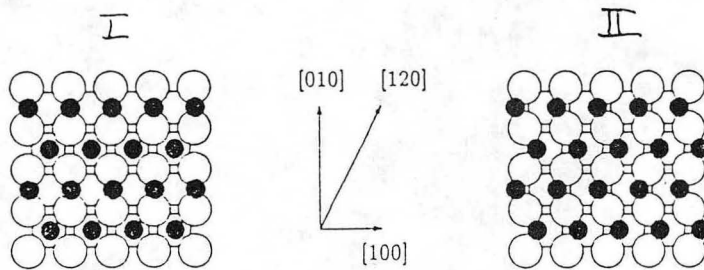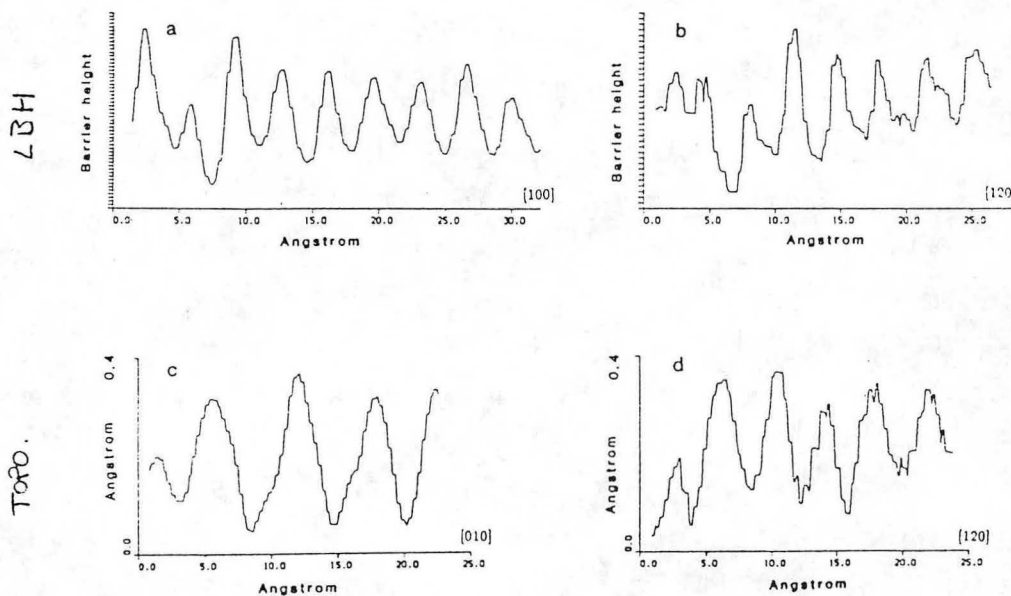
Structure II favored

XBL 881-115

Fig. 4
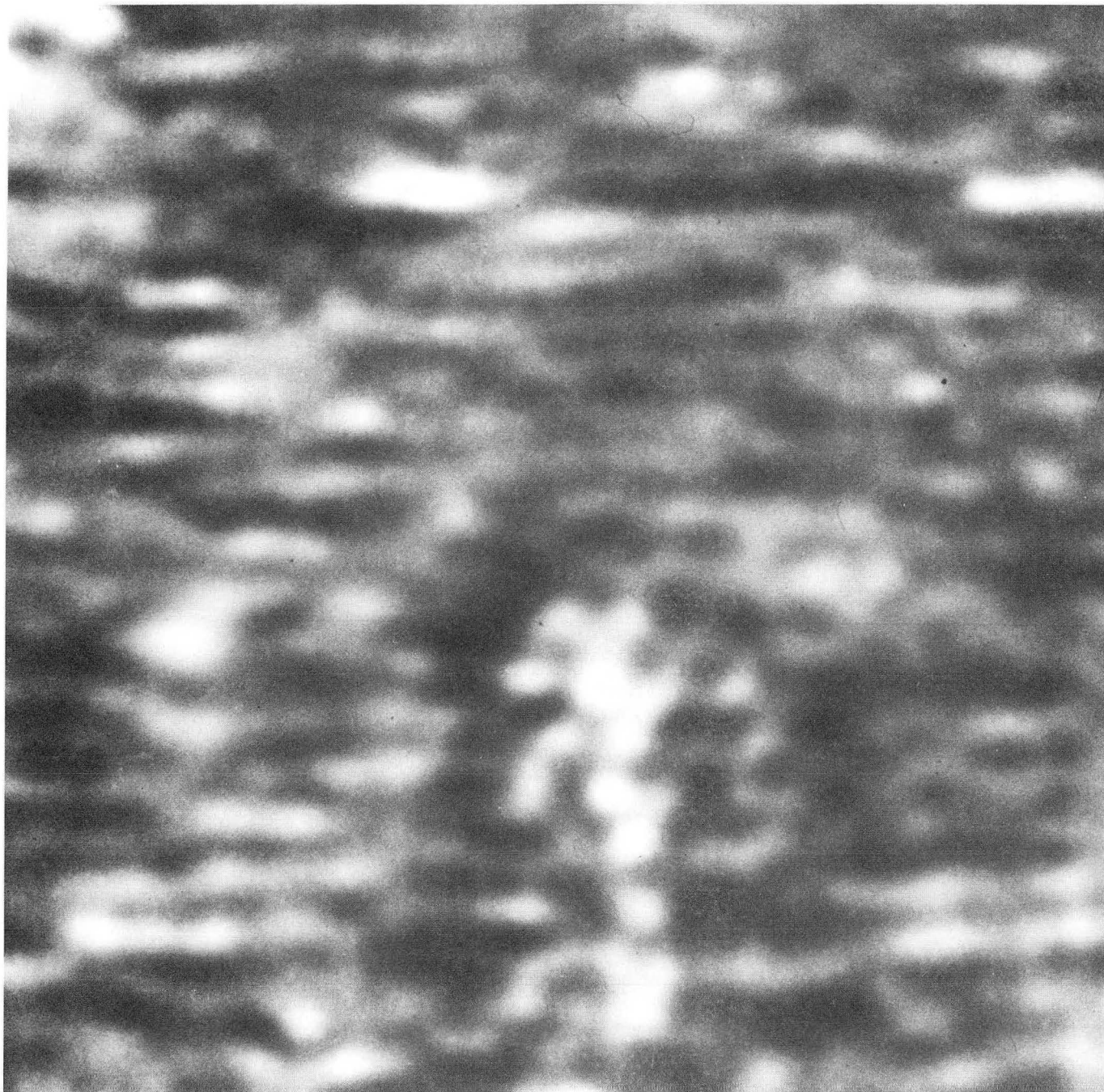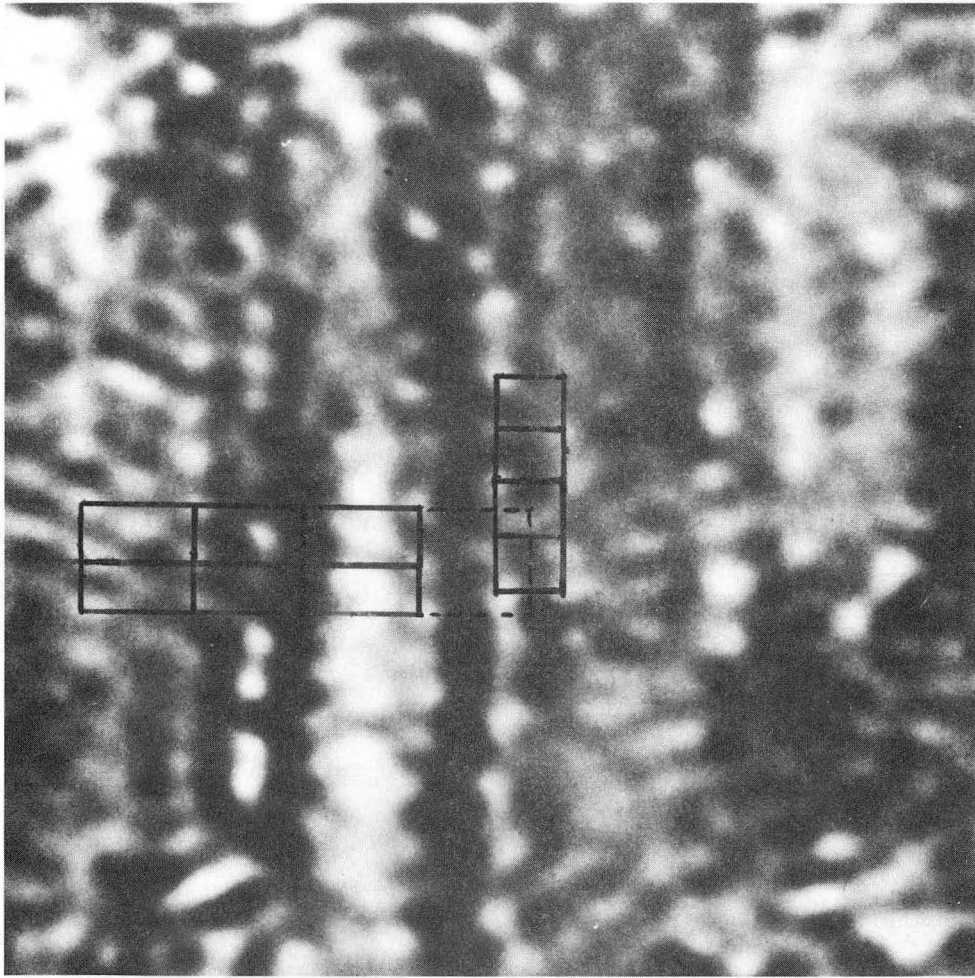
XBB 886-6621

Fig. 5
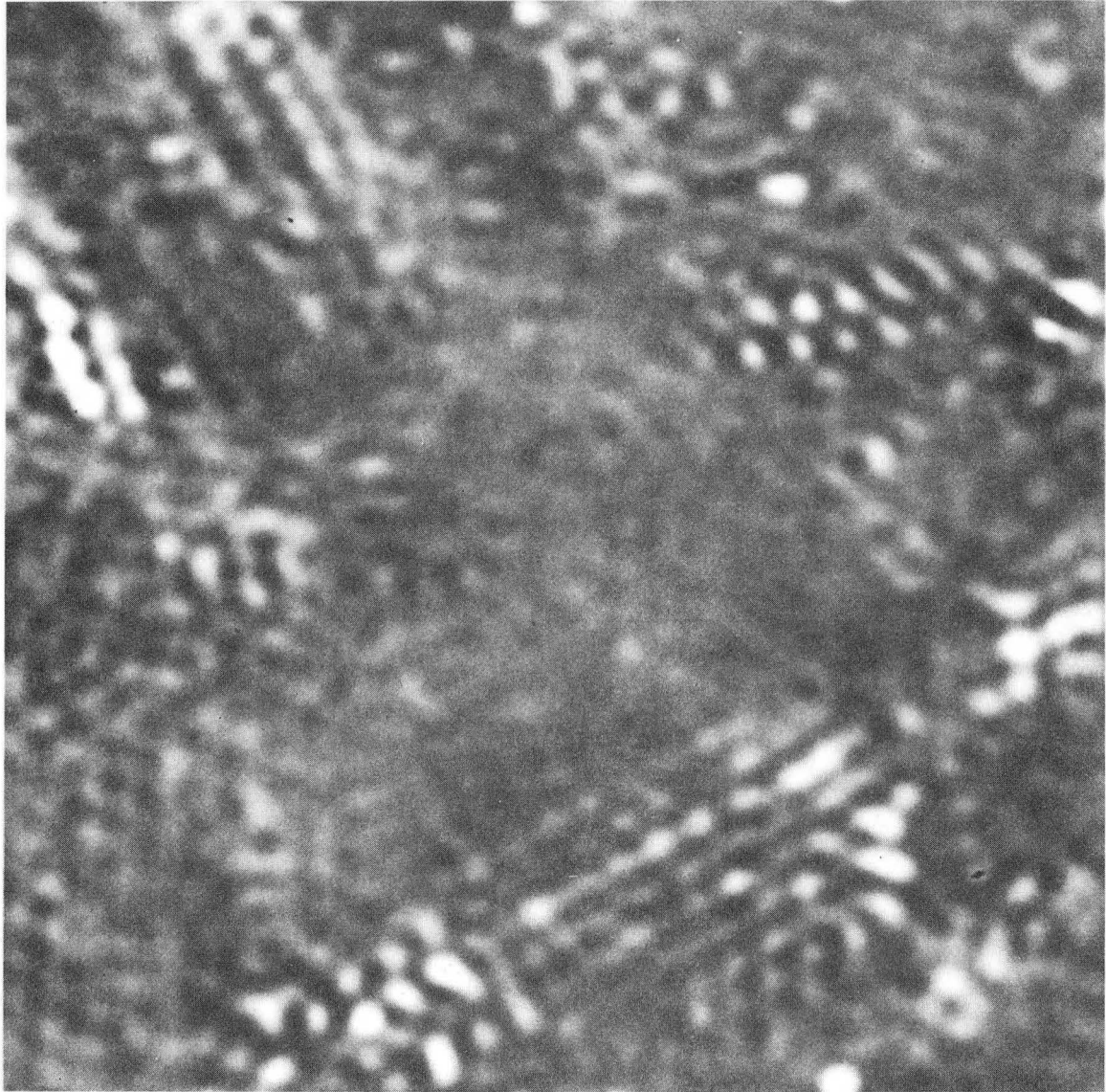
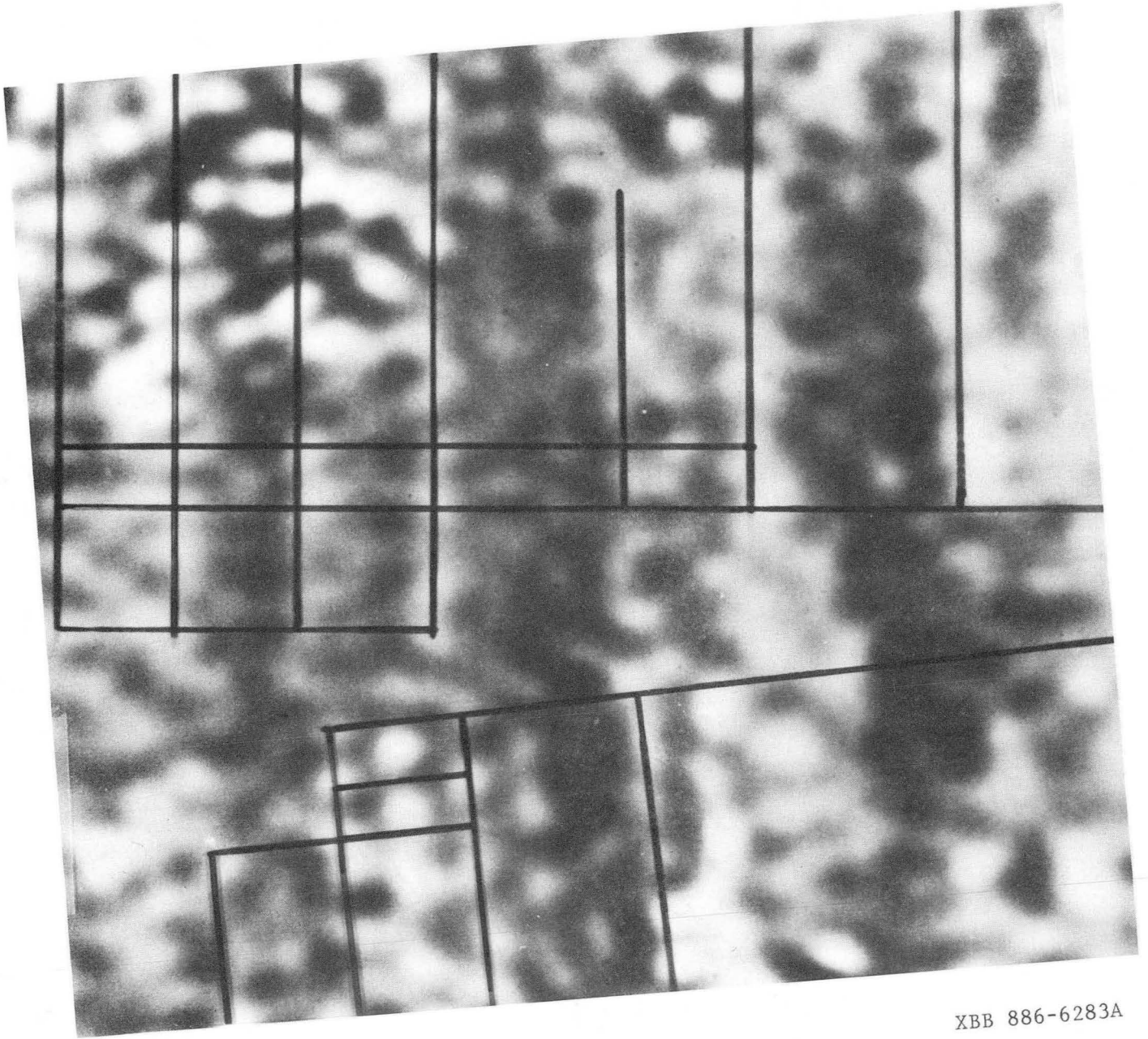XBB 886-6284

Fig. 6
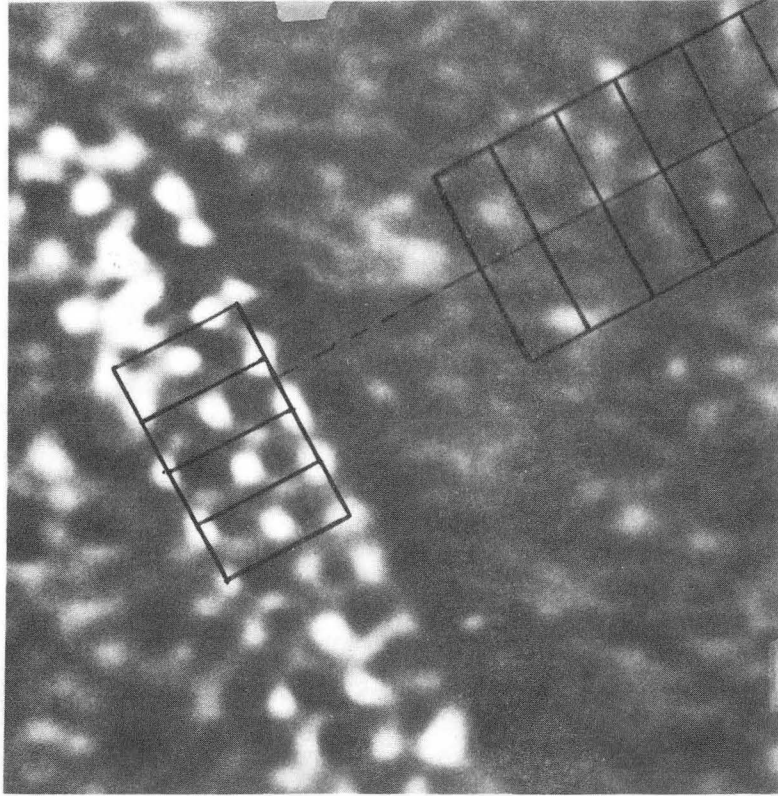
XBB 886-6287A
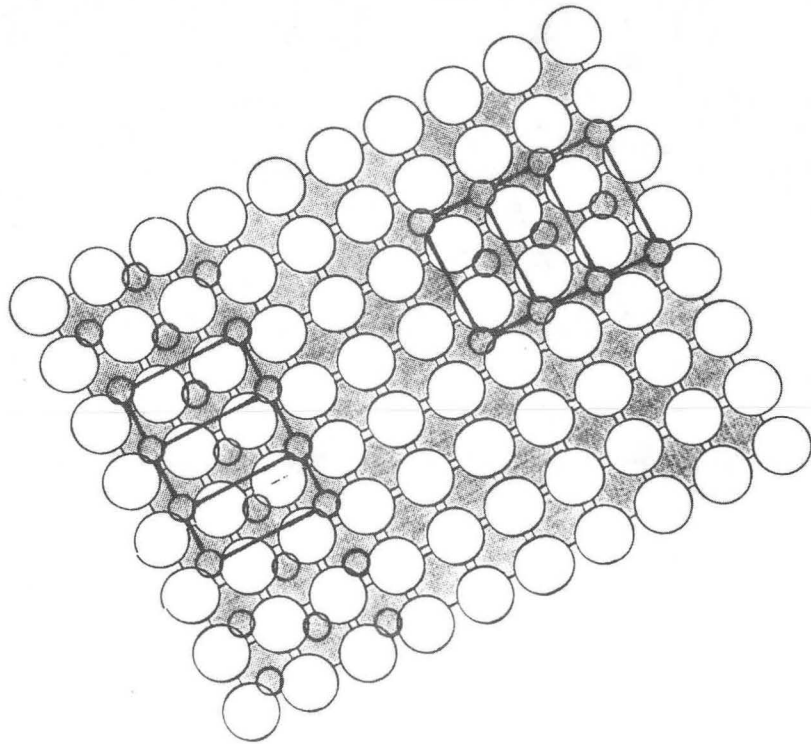
Fig. 7

XBB 886-6290A
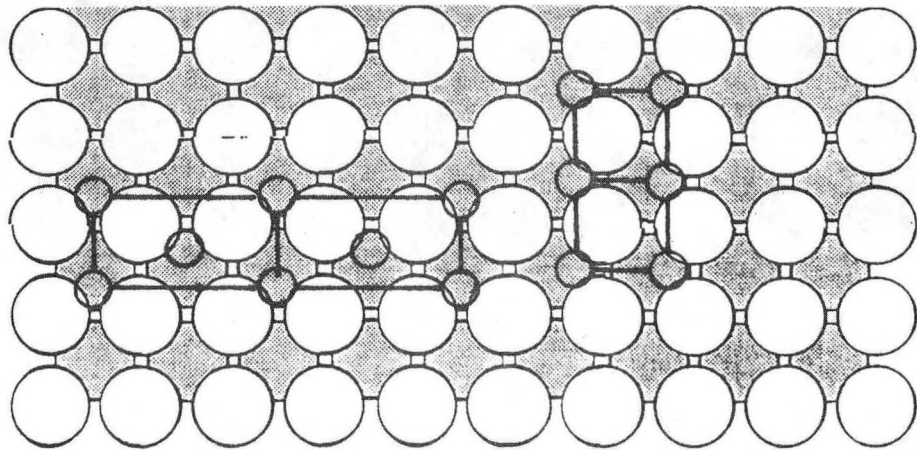
Fig. 8

XBB 886-6283A

Fig. 9

XBB 886-6471

Fig. 10